Workflow: Annotated pdf

PROOF COVER SHEET

Author(s): Nicolás Tenaglia
Article title: Study of shrinkage porosity in spheroidal graphite cast iron
Article no: YCMR 1106783
Enclosures: 1) Query sheet
2) Article proofs

Dear Author,

Please find attached the proofs for your article.

1. Please check these proofs carefully. It is the responsibility of the corresponding author to check these and approve or amend them. A second proof is not normally provided. Taylor & Francis cannot be held responsible for uncorrected errors, even if introduced during the production process. Once your corrections have been added to the article, it will be considered ready for publication

Please limit changes at this stage to the correction of errors. You should not make trivial changes, improve prose style, add new material, or delete existing material at this stage. You may be charged if your corrections are excessive (we would not expect corrections to exceed 30 changes).

For detailed guidance on how to check your proofs, please paste this address into a new browser window: http://journalauthors.tandf.co.uk/production/checkingproofs.asp

Your PDF proof file has been enabled so that you can comment on the proof directly using Adobe Acrobat. If you wish to do this, please save the file to your hard disk first. For further information on marking corrections using Acrobat, please paste this address into a new browser window:http://journalauthors.tandf.co.uk/production/acrobat.asp

2. Please review the table of contributors below and confirm that the first and last names are structured correctly and that the authors are listed in the correct order of contribution. This check is to ensure that your names will appear correctly online and when the article is indexed.

Sequence	Prefix	Given name(s)	Surname	Suffix
1		Nicolás	Tenaglia	
2		Roberto	Boeri	
3		Graciela	Rivera	
4		Juan	Massone	

Queries are marked in the margins of the proofs, and you can also click the hyperlinks below.

AUTHOR QUERIES

General points:

1. **Permissions:** You have warranted that you have secured the necessary written permission from the appropriate copyright owner for the reproduction of any text, illustration, or other material in your article. For further guidance on this topic please see: http://journalauthors.tandf.co.uk/copyright/usingThirdPartyMaterial.asp
2. **Third-party material:** If there is material in your article that is owned by a third party, please check that the necessary details of the copyright/rights owner are shown correctly.
3. **Affiliation:** The corresponding author is responsible for ensuring that address and email details are correct for all the co-authors. Affiliations given in the article should be the affiliation at the time the research was conducted. For further guidance on this topic please see: http://journalauthors.tandf.co.uk/preparation/writing.asp.
4. **Funding:** Was your research for this article funded by a funding agency? If so, please insert 'This work was supported by <insert the name of the funding agency in full>', followed by the grant number in square brackets '[grant number xxxx]'.
5. **Supplemental data and underlying research materials:** Do you wish to include the location of the underlying research materials (e.g. data, samples or models) for your article? If so, please insert this sentence before the reference section: 'The underlying research materials for this article can be accessed at <full link>/ description of location [author to complete]'. If your article includes supplemental data, the link will also be provided in this paragraph. See <http://journalauthors.tandf.co.uk/preparation/multimedia.asp> for further explanation of supplemental data and underlying research materials.

AQ1	Please check the short title that has been created, or suggest an alternative title.
AQ2	Please provide missing volume number for Ref. [7].
AQ3	Please supply a caption for figures 1–13.

How to make corrections to your proofs using Adobe Acrobat/Reader

Taylor & Francis offers you a choice of options to help you make corrections to your proofs. Your PDF proof file has been enabled so that you can mark up the proof directly using Adobe Acrobat/Reader. This is the simplest and best way for you to ensure that your corrections will be incorporated. If you wish to do this, please follow these instructions:

1. Save the file to your hard disk.

2. Check which version of Adobe Acrobat/Reader you have on your computer. You can do this by clicking on the "Help" tab, and then "About".

   If Adobe Reader is not installed, you can get the latest version free from http://get.adobe.com/reader/.

3. If you have Adobe Acrobat/Reader 10 or a later version, click on the "Comment" link at the right-hand side to view the Comments pane.

4. You can then select any text and mark it up for deletion or replacement, or insert new text as needed. Please note that these will clearly be displayed in the Comments pane and secondary annotation is not needed to draw attention to your corrections. If you need to include new sections of text, it is also possible to add a comment to the proofs. To do this, use the Sticky Note tool in the task bar. Please also see our FAQs here: http://journalauthors.tandf.co.uk/ production/index.asp.

5. Make sure that you save the file when you close the document before uploading it to CATS using the "Upload File" button on the online correction form. If you have more than one file, please zip them together and then upload the zip file.

   If you prefer, you can make your corrections using the CATS online correction form.

Troubleshooting

Acrobat help:http://helpx.adobe.com/acrobat.html
Reader help:http://helpx.adobe.com/reader.html

Please note that full user guides for earlier versions of these programs are available from the Adobe Help pages by clicking on the link "Previous versions" under the "Help and tutorials" heading from the relevant link above. Commenting functionality is available from Adobe Reader 8.0 onwards and from Adobe Acrobat 7.0 onwards.

Firefox users: Firefox's inbuilt PDF Viewer is set to the default; please see the following for instructions on how to use this and download the PDF to your hard drive:
http://support.mozilla.org/en-US/kb/view-pdf-files-firefox-without-downloading-them#w_using-a-pdf-reader-plugin

Study of shrinkage porosity in spheroidal graphite cast iron

Nicolás Tenaglia*, Roberto Boeri, Graciela Rivera and Juan Massone

This study aims at identifying the relationship between the shrinkage cavities and the solidification structure in spheroidal graphite cast iron. Cast samples specially designed to contain shrinkage cavities were used. The solidification macrostructure was revealed using the Direct Austempering After Solidification method, while the solidification microstructure was revealed by using colour etching. At the midsection of the pieces, the shrinkage cavities and the solidification structure were observed jointly. The study showed that the classification of shrinkage porosity found in literature does not correspond to the ductile iron solidification model recognized by most of the scientific community. Early solidification models, and therefore shrinkage formation mechanisms, were proposed in instances when there was not a thorough knowledge of the morphology of the solid phases during solidification. Nowadays, defects formation mechanisms can be described with higher accuracy. Therefore, an updated classification of shrinkage porosity for spheroidal graphite iron is proposed.

Keywords: Ductile iron, Solidification structure, Shrinkage porosity

Introduction

Spheroidal graphite cast iron (SGI) or ductile iron is a material widely used to manufacture a large number of mechanical parts. The main favourable characteristics of SGI include its ease of moulding and posterior machining, high availability and low cost of raw materials and the variety of heat treatments that can be used to improve its mechanical properties. However, the increasing demand on the properties of the finished products, along with the pressure to reduce costs, create a great need to consistently produce better quality castings. A major problem affecting SGI castings are shrinkage defects that occur during the solidification and subsequent cooling in the casting. Shrinkage often leads to the rejection of the parts. When high strength pieces are produced, it is critical to ensure that they are structurally sound. Avoiding the presence of microshrinkage demands a thorough understanding of its origin.

Recent experiments have shown that the ductile iron macrostructure, formed during solidification, is characterized by the formation of large austenite dendrites. The macrostructure can be revealed to the naked eye using a special technique referred to as Direct Austempering After Solidification method (DAAS).[1–3] The microstructural characteristics can be revealed by conventional and colour metallography techniques. The examination after regular etching can characterize the quantity, size and morphology of graphite and the phases forming the metallic matrix, while the use of proper colour etching reagents can reveal the distribution and extension of last to freeze zones (LTF) through the identification of the microsegregation patterns. The joint analysis of macro and microscopic features allows a comprehensive characterization of ductile iron structure.

INTEMA, UNMdP – CONICET, Mar del Plata, Argentina

*Corresponding author, email ntenaglia@fi.mdp.edu.ar

Solidification processes can be accompanied by defect formation such as shrinkage cavities. Stefanescu[4] proposed a classic classification of shrinkage defects (Fig. 1). In principle, three different types of shrinkage cavities can be formed in a casting: (a) the concentrated shrinkage; (b) the dispersed macroshrinkage, and (c) the dispersed microshrinkage. Concentrated shrinkage forms because of metal contraction during cooling of the liquid and the phase change. It can be open or closed to the atmosphere.

The dispersed macroshrinkage consists of cavities of millimetre size resulting from the lack of feeding during solidification. It appears in heavy sections or at hot spots of the casting and could be eliminated through the optimization of the riser design. Macroshrinkage usually appears either as isolated or as interconnected irregular cavities that can be observed with the naked eye on a cross section of the casting. The cavity walls are rough.

The microshrinkage is usually dispersed in the whole volume of the casting. It consists of micron-size cavities that are formed between the eutectic grains or dendrite arms at the end of the eutectic solidification. It can be observed only using microscopes.

The objective of this investigation was to study the correlation of the solidification structure of SGI with the formation of shrinkage cavities, in an attempt to gain a better understanding of the origin of macro and microshrinkage cavities. Concentrated shrinkage cavities will not be studied in this work.

Experimental procedure

Casting sample

The sample used in this work was designed with the following objectives:

- To obtain macro and microporosity in the pieces.

Received 11 March 2015 Accepted 14 September 2015
DOI 10.1080/13640461.2015.1106783

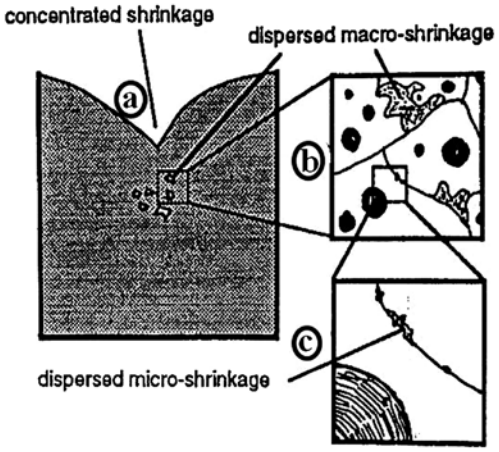

AQ3 1

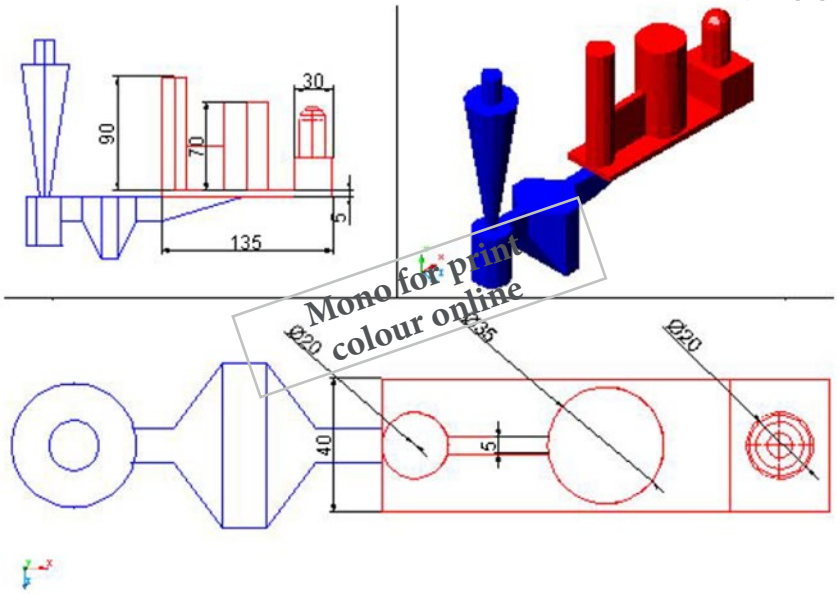

2

- To allow hot shakeout when the temperature of the entire part is above the higher limit of the upper intercritical temperature range (T_{cu}) of the Fe–C–Si diagram, where α, γ, and graphite coexist (DAAS technique).
- To allow correct feeding to the entire piece, ensuring a non-turbulent filling.

In the first design, dimensions and geometric relations that violate the rules of good art were used intentionally, such as right angles; hot spots; intricate areas with feeding difficulty; abrupt changes in section size; zones of low metallostatic pressure; long feeder roads; thin sections, among others. The solidification of a casting corresponding to the proposed design was then simulated using the MagmaSoft® software, making further adjustments to the geometry in order to maintain the presence of micro-cavities and to obtain the temperature profile required by the DAAS technique.

For the prediction of shrinkage porosity, MagmaSoft criteria called Soundness, Porosity and Hot Spots were used. For proper filling, the filling speed and temperature criteria were followed during the simulations, attempting to obtain in all cases filling rates below 1 m s^{-1} in order to avoid turbulent flow, and filling temperatures above the liquidus to avoid the flow of metal in mushy condition

In order to guarantee that the temperature of every point of the parts is above T_{cu} at the time of shake out, T_{cu} was calculated using the following equation[5]:

$$T_{CU}(°C) = 723 - 0.3 \times \text{wt\%C} + 43 \times \text{wt\%Si} - 33 \times \text{wt\%Mn} - 6 \times \text{wt\%Cu} \quad (1)$$

The simulations were performed using the properties of nodular iron eutectic GJS-600 listed in the MagmaSoft database with the following temperatures:

- Liquidus temperature = 1169 °C
- Solidus temperature = 1166 °C

Other simulation parameters employed were:

- Filling temperature = 1360 °C
- Filling time = 5 s.
- Feeding efficiency = 70%
- Inoculation treatment = 70%
- Graphite precipitation = 7
- Silica-dry mould at 25 °C.

For the chemical composition of GJS-600 on the MagmaSoft database (wt% 3.6C-2.55Si-0.12Mn-0.016P-0.6Cu-0.05Mg) T_{cu} is 824 °C. A conservative value of temperature of 850 °C was adopted as the minimum acceptable for shake out. During the simulations both liquid fraction and the

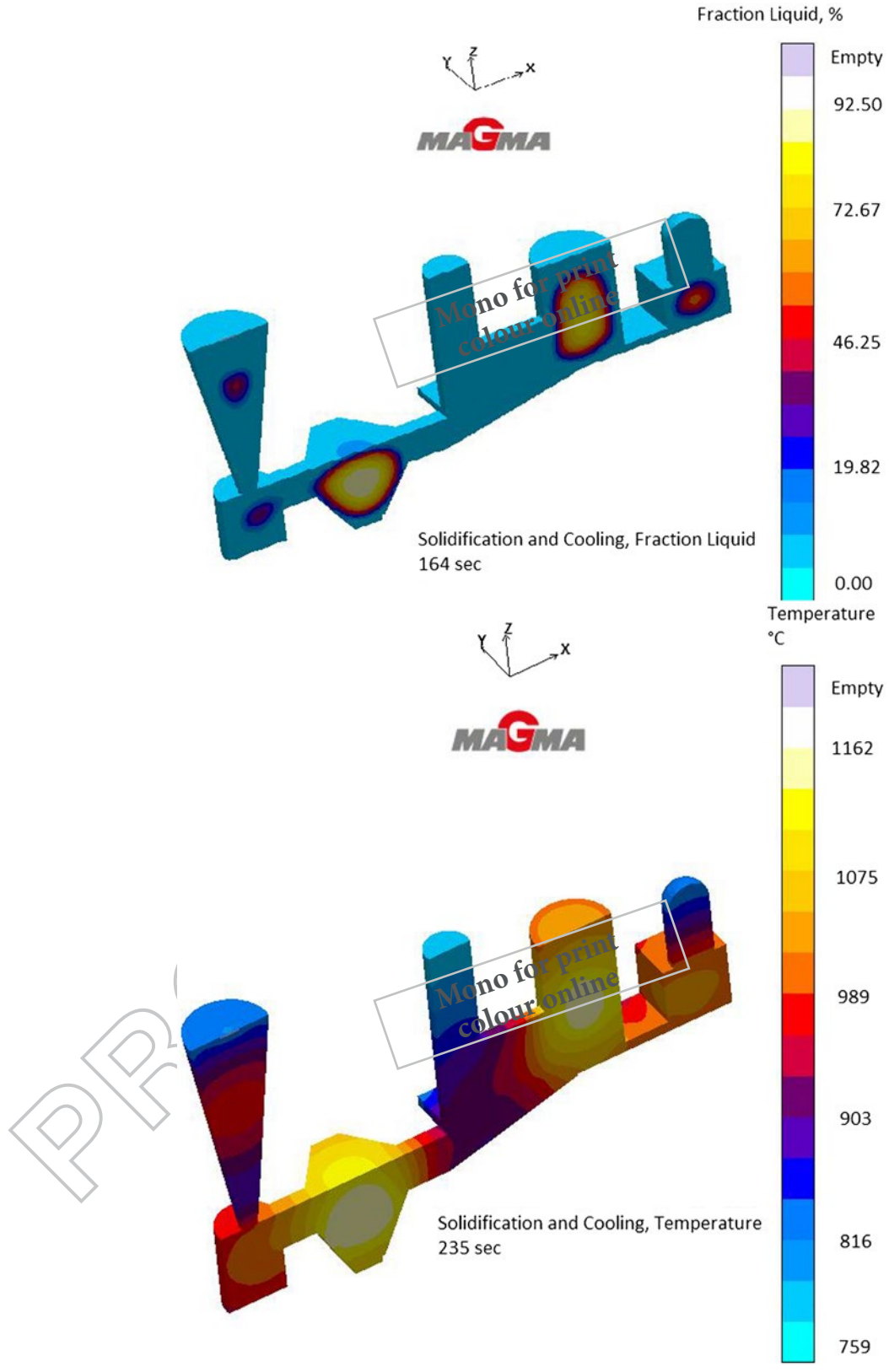

3

temperature are monitored, seeking to define a time interval ranging from the time at which the sample has developed a thick solidified layer, to the time at which the temperature is above 850 °C at all points of the part.

Figure 2 shows a schematic drawing of the part designed.

The shakeout time is defined as the time elapsed from the completion of the filling of the mould so that the piece is at the right temperature for mould opening and the implementation of the DAAS technique. This time is dependent on the pouring temperature, which is assumed at 1360 °C. Figure 3-1 shows that a significant solid layer is formed after 164 s from the start of pouring. Figure 3-2 shows that the temperature is above 850 °C at all points after 235 s. These time values define the interval along which the shakeout is possible.

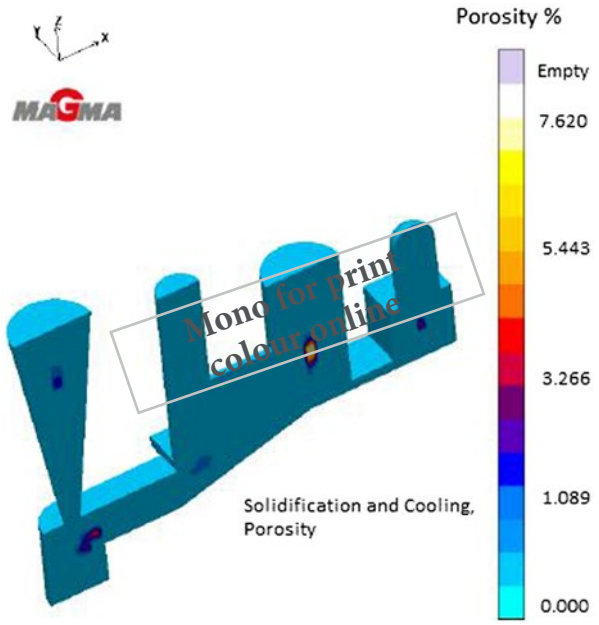

4

Table 1 Chemical composition

%C	%Si	%Mn	%S	%P	%Mg	%Cu	%Ni
3.31	2.76	0.13	0.021	0.039	0.053	0.85	0.53

Figure 4 shows the predicted profile of porosity at the middle section of the casting. As intended, different portions of the casting show shrinkage defects.

Material

Melt was prepared using a 50-kg capacity medium-frequency induction furnace. Pig iron, steel scrap, ferroalloys and carbon raiser were used as raw materials in order to obtain ductile iron with near-eutectic chemical composition. Also, the melt was alloyed with nickel and copper to attain sufficient austemperability to carry out the DAAS technique. The melt was treated with 1.6% of Fe–Si-(9%)Mg and inoculated with 0.65% Fe–Si(75%). Moulds were made using resin-bonded silica sand. Table 1 lists the chemical composition of the melt.

The T_{cu} of this melt, as calculated by Eq. 1, is 830 °C, not very different from the value for GJS-600. Therefore, the same time interval for shake out was used in the experiments.

Revealing of solidification macro and microstructures

The solidification macrostructure was revealed by applying the DAAS technique. It consists of an austempering heat treatment that must be carried out immediately after solidification, which leads to the formation of an ausferritic microstructure (mix of ferrite and retained austenite). The retained austenite is the primary phase. After etching, austenite grains are revealed macroscopically. A detailed description of the technique can be found elsewhere[2]. In this study, the parts were shaken out after 180 s from full filling. Then the parts were quickly transferred to an electric furnace held at 900 °C, where they were maintained for 30 min to stabilize the temperature. An austempering treatment was then performed in a molten salt bath held at 360 °C for 60 min.

The solidification microstructure was revealed by a colour etching technique.[2] Specimens were previously ferritized to improve etching efficiency, as recommended in the literature.[6] Etchant consisted of 10 g of NaOH, 40 g of KOH, 10 g of picric acid and 50 ml of distilled water and must be applied while boiling.

Results and discussion

The solidification macrostructure obtained at the cross section of one specimen is shown in Fig. 5. The piece was sectioned, ground, polished and etched with Nital. A typical grained structure can be seen, characterized by the presence of equiaxed and columnar grains. The central part of the sample displays some orange colouring that is caused by an oxidation induced by the presence of dispersed shrinkage.

When the colour etching is applied in order to reveal the solidification microstructure (Fig. 6) most of the sample surface shows green colouration, while some zones appear as isolated portions of yellow colouration, surrounded by red and blue halos. One of these zones is pointed by white arrows in Fig. 6. These isolated portions are Si depleted zones, which correspond with the LTF portions of melt. It is important to recognize that the colouration of each zone depends on the etching time, however colour sequences (from first to LTF zones) are always the same: yellow, green, blue, red and yellow again.

According to the solidification model of SGI proposed originally by Rickert and Engler[7] and later on adopted and experimentally improved by Rivera *et al.*[2] austenite and graphite nodules nucleate independently in the liquid. As

5

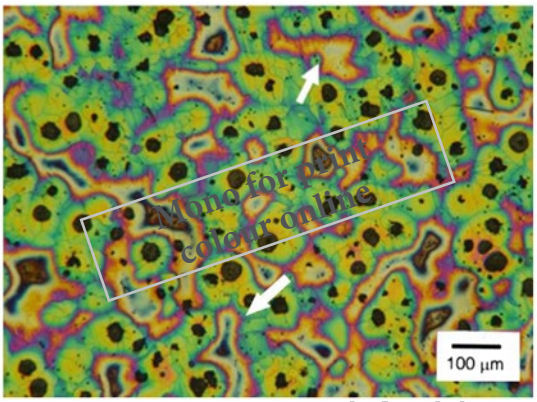

6

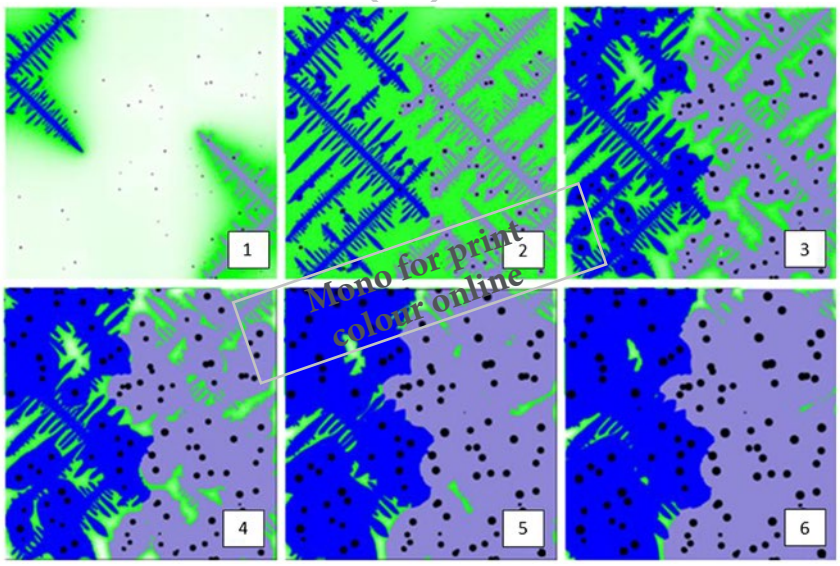

7

the solid fraction increases, the austenite grows dendritically touching and enveloping the graphite nodules. The advance of the austenite dendrites leaves significant amounts of liquid between the secondary arms. In this manner, at the point at which dendrite coherence is reached, defining the grain size, there are still "liquid pockets" inside each grain. This process can be described graphically in good detail using the 2D drawing of Fig. 7 which shows a sequence of the interaction of two dendrites of austenite and graphite spheroids[8] during the solidification progress. Near the completion of solidification the last portions of melt are located within the dendrite arms, as shown in Fig. 7-5 and 7-6 (green areas). Ideally, as solidification proceeds austenite dendrite branches coarsen and the graphite spheroids continue to grow enveloped in austenite. Nevertheless, in the actual solidification, some regions of the sample may show limited liquid feeding, especially after dendrites coherence, resulting in empty volumes called dispersed shrinkage porosity.

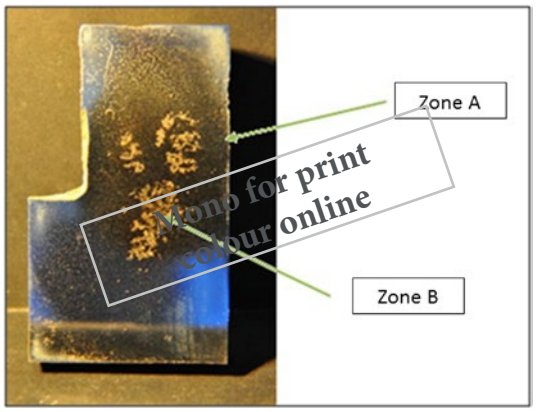

8

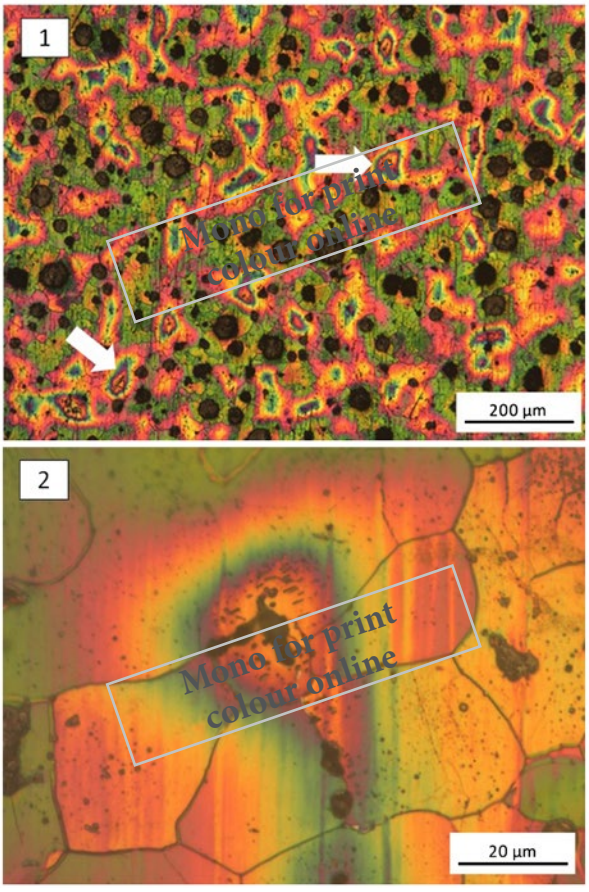

9

Figure 8 shows the polished surface of one of the samples. A defective area (B), and an apparently sound area (A) can be identified.

Zone A analysis

Zone A is located near the sample surface, therefore it will solidify early and the liquid feeding to the local LTF zones should be sufficient to prevent the formation of shrinkage cavities. The macroscopic examination reveals no dispersed shrinkage porosity. Nevertheless, when careful microscopic examination is carried out, very small and dispersed shrinkage (microshrinkage) cavities can be identified, as shown in Fig. 9 after colour etching. In Fig. 9-1 the arrows point at microshrinkage cavities, which are surrounded by yellow, green, red and orange halos, suggesting that they locate at a LTF zone. Figure 9-2 shows a higher magnification image of a microshrinkage cavity.

Zone B analysis

Zone B locates at a thermal or geometrical centre of the casting, therefore it will be the macroscopic LTF zone. At such location, feeding is less efficient than in zone A because by the time of completing the solidification, thermal centres are surrounded by solid material and the liquid

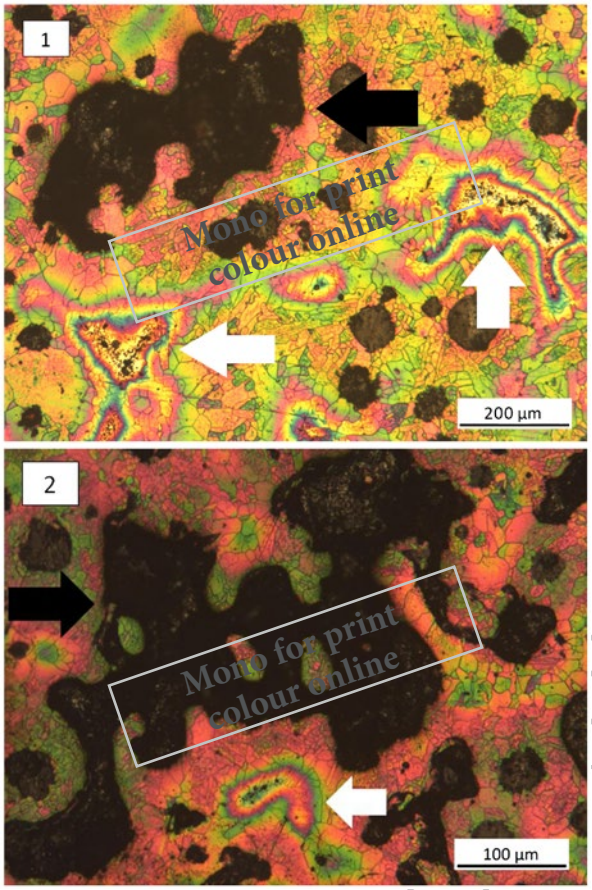

10

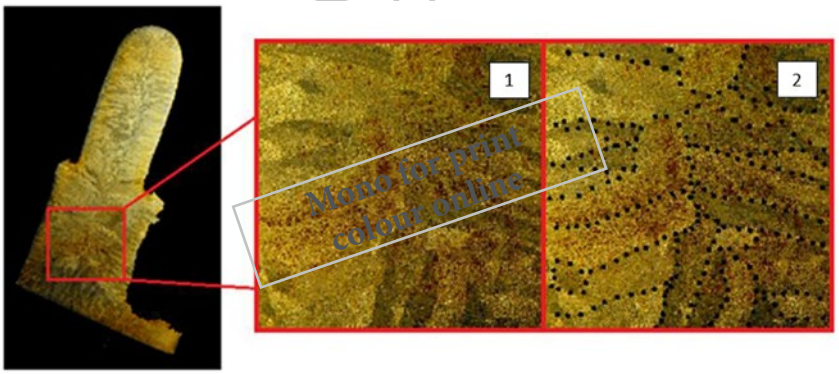

11

cannot flow from feeders to compensate contraction. Colour etching of these zones is shown in Figs. 10-1 and 10-2 at higher magnification. It is possible to identify shrinkage cavities of two different extents. Some small and dispersed microshrinkages located at some LTF zones (indicated by white arrows in Fig. 10) are similar to those observed at zone A. In addition, other larger cavities (dispersed macroshrinkage) which are not surrounded by coloured halos are also observed and pointed by black arrows in Fig. 10. This suggests that the larger dispersed porosity is formed at a stage in which the remaining liquid phase exhibits no marked microsegregation.

It is important to note that the dispersed porosity is mostly intragranular. This characteristic can be observed clearly in Fig. 11. Figure 11-1 shows the solidification macrostructure in zone B obtained by the DAAS technique and Nital (2%) etchant. Red areas correspond to rusty porosity. In Fig. 11-2, the grain boundaries have been remarked by dots to improve the observation. It is clear that the shrinkage porosity develops within a grain or a primary austenite dendrite; therefore, it will be referred to as "intradendritic".

Figure 12 shows the dispersed shrinkage porosity, observed by SEM. The intradendritic nature of cavities is evident by observing that their walls are conformed by dendrite arms.

Figure 13 shows a summary of the different types of internal shrinkage porosity that may be present in a ductile iron cast part. Figure 13 (left) shows the midsection of one of the samples submitted to DAAS and etched with Nital (2%), where the macrostructure is revealed. A higher magnification view of the centre of the sample shows some grains with red

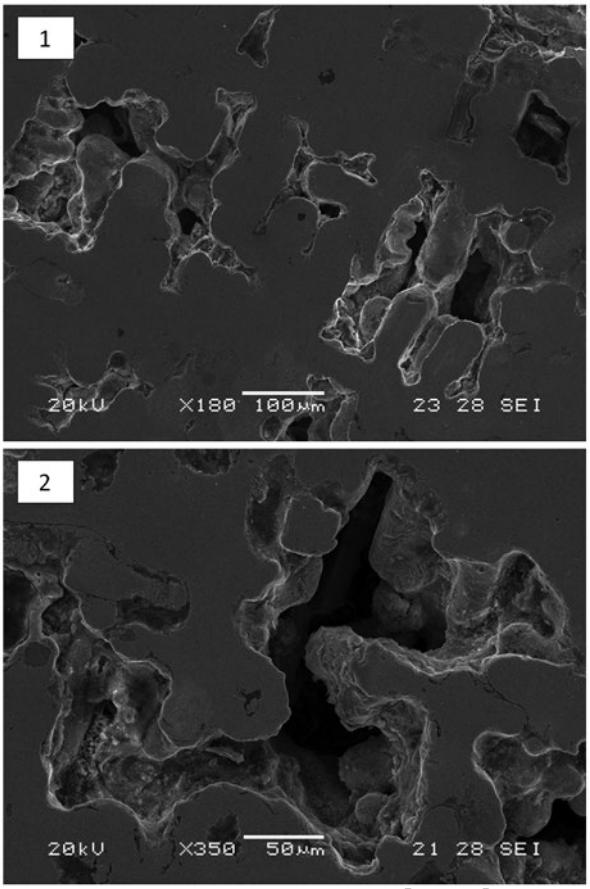

12

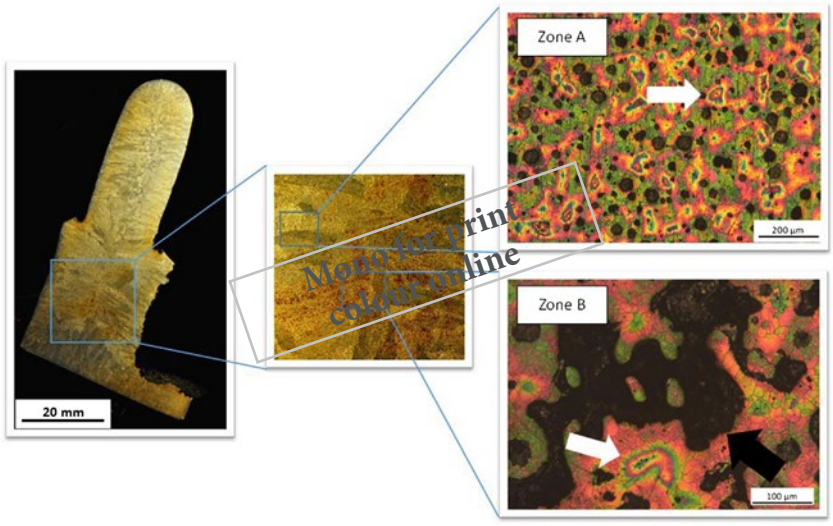

13

spots, caused by the intense attack of the Nital when shrinkage cavities are present. Two different types of zones can be marked, one showing grains apparently free from corrosion spots (zone A), and zones having corroded grains (zone B). Higher magnification observations after colour etching (right of Fig. 13) shows that only very small microshrinkage cavities (noted by the sequence of colours surrounding them and pointed by white arrows) are present in zone A. On the other hand, zone B, corresponding to the thermal centre of the sample, shows both dispersed macroshrinkage (black arrow) and microshrinkage (white arrows).

These results support the proposal of a classification of the shrinkage cavities in spheroidal cast iron as follows:

- Concentrated macroshrinkage (not observed in the image): defect that occurs by a material deficit because of contractions in liquid state and phase change. It can be open or closed to the atmosphere. This definition coincides with that of the literature.

- Dispersed macroshrinkage: defect that locates at the thermal centres of the casting. At macroscopic scale, it is possible to observe an agglomeration of cavities that can occupy some millimetres. The microscopic examination reveals the intradendritic nature of its shape, having sizes of about 200 μm for the present experimental conditions. When the surroundings of the cavities are observed after colour etching, they do not appear to be surrounded by coloured halos, suggesting that they form from a liquid that is not highly segregated. Nevertheless, this hypothesis remains to be proved experimentally.
- Dispersed microshrinkage: defects of about 10–20 μm that locate at LTF zones, showing an intense microsegregation at their surroundings. It is proposed that their formation process is similar to that of dispersed macroporosity, but in this case feeding is interrupted at a very advanced stage of solidification, and the porosity reaches very small dimensions. They are typically intragranular or intradendritic, and can be present along the entire piece.

Conclusions

(1) The combined observation of the macrostructure and the microstructure of samples of spheroidal cast iron showing the presence of shrinkage defects has allowed to identify the location of the macro and microshrinkage defects with respect to the solidification structure.

(2) Dispersed macroshrinkage cavities develop inside solidification units or primary austenite grains.

(3) Dispersed microshrinkage cavities develop along similar areas than dispersed macroshrinkage, but creating much smaller cavities in coincidence with LTF zones. They form along areas of greater microsegregation.

(4) The contraction defects classification was updated for SGI.

Acknowledgement

The study made use of an academic licence of MagmaSoft, which is gratefully acknowledged.

References

1. G. Rivera, R. Boeri and J. Sikora. *Key Eng. Mater.* 2011, **457**, 67–72.
2. G. Rivera, R. Boeri and J. Sikora. *Mater. Sci. Technol.* 2002, **18**, 691–697.
3. G. Rivera, P. R. Calvillo, R. Boeri, Y. Houbaert and J. Sikora. *Mater. Charact.* 2008, **59**, 1342–1348.
4. D. M. Stefanescu, H. Q. Qiu and C. H. Chen. *AFS Trans.* 1995, **57**, 189–197.
5. I. Galarreta, R. Boeri and J. Sikora. *Int. J. Cast Metals Res.* 1997, **9**, 353–358.
6. G. Rivera, R. Boeri and J. Sikora. *Cast Metals* 1995, **8**, 1–5.
7. A. Rickert and S. Engler. *Mater. Res. Soc. Proc.* 1985, 165–174.
8. E. Fras, D. Gurgul, J. Sikora, A. Burbelko and W. Kapturkiewicz. 9th International Symposium on Science and Processing of Cast Iron, SPCI-9, Egypt, Luxor, 2010.